Revista de Chimie
https://revistadechimie.ro
https://doi.org/10.37358/Rev.Chim.1949

Experimental Studies Regarding the Distribution of the Masticatory Pressures According to the Turn's Length of the Dental Implants

ALEXANDRU DANIEL REFERENDARU[1], ANCA IULIANA POPESCU[2], IASMIN MIREA[1], STEFANIA ANDRADA IANCU[1], RALUCA MONICA COMANEANU[2*], HORIA MIHAIL BARBU[2]
[1] Titu Maiorescu Doctoral School of Dental Medicine, 22 Dambovnicului Str., 040441, Bucharest, Romania
[2] Titu Maiorescu University of Bucharest, Faculty of Dental Medicine, 67A Gh. Petrascu Str., 031593, Bucharest, Romania

Abstract. *In order to study comparatively the behaviour of the bone-implant interface at mechanical stresses depending on the length of the implant turns, we chose a complex case, a total bimaxillary edentate. 7 implants were virtually inserted into the maxilla (2 pterigoid implants in the lateral regions and 3 implants in the frontal region), and 4 implants were inserted into the mandible (two in the premolar regions and two corresponding to the canines). The FEA analyzes were performed separately for the maxilla and for the mandible, applying a force of 200N on each type of implant. The critical areas, in which the extreme values of the strains develop, are located into the bone on the neck-implant level, and its apex level, regardless of the type of implant and regardless of the maxillary or mandibular area where the implants were virtually inserted. Implants with small turns induce lower stresses and deformations, compared to implants with large turns.*

Keywords: *FEA, dental implants, short turns, long turns*

1.Introduction

The rehabilitation of the edentulous jaws with the help of dental implants is now considered a safe therapeutic possibility [1], which can offer patients the restoration of the structures of the dental-maxillary apparatus from an aesthetic and functional point of view. The use of a fixed prosthetic superstructure, aggregated by screwing or a movable over-prosthesis applied over a conjunction bar can be considered treatment variants for an edentulous patient with marked maxillary bone atrophy. [2, 3] In the case of a fixed prosthetic superstructure aggregated by screwing, the fracture of the prosthetic restoration or the fracture of one of the fixing screws may occur, followed by a peri-implantar bone loss, associated with the inflammation of the soft and hard tissues around the implant [4, 5].

Finite element analysis is an currently experimental method used more and more frequently in the field of dental medicine [6-21] to estimate the behaviour of biomaterials and human tissues. The use of engineering expertise in dentistry has partly helped to understand the biomechanical aspects related to the osseointegration of the implants [1]. However, at the present moment, the mechanisms responsible for the lack of implant integration, the therapeutic failure or the fracture of the components, are not yet fully known and the internationally reported data about the influence of some biomechanical parameters are not very conclusive [22], which justifies the further analysis of the different types of edentulous and implants for a better characterization and justification of the phenomena occurring at the bone-implant interface.

2. Materials and methods

In order to study comparatively the behavior of the bone-implant interface at mechanical stresses depending on the length of the implant turns, we chose a complex case, a total bimaxillary edentate. The patient's CBCT was imported into Mimics Innovation Suite 17, Materialise NV© and processed. After processing, 7 implants were virtually inserted into the maxilla (2 pterigoid implants in the lateral regions and 3 implants in the frontal region), and 4 implants were inserted into the mandible (two in the premolar

**email: monica_tarcolea@yahoo.co.uk* *All authors have equal contributions to the study.*

regions and two corresponding to the canines) (Figure 1). Within the study, the 3 implants inserted into the frontal maxillar region and the 4 mandibular implants were considered initially with large turns, subsequent with small turns, in order to detect possible differences in the bone-implant interface depending on the implant design, respectively the size of their turns.

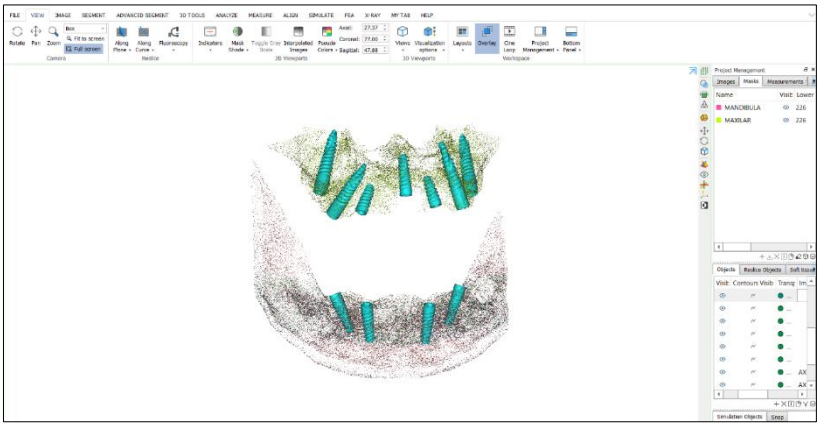

Figure 1. The positions where the implants were virtually inserted

Mastication stress simulations were performed with ANSYS 16, ANSYS Inc©. The analyzes were performed separately for the maxilla and for the mandible, applying a force of 200N on each type of implant. Considering the particular situation of the patient, with advanced bone resorption and with increased porosity of the residual ridges, higher values of the mastication force were not discussed. The properties of the materials used in the simulations are presented in Table 1.

Table 1. The TiAlV alloy, mandibular bone and maxillary bone used in simulations

	Young's Modulus MPa	Poisson's Ratio	Bulk Modulus MPa	Shear Modulus MPa
TiAlV alloy	1.e+005	0.3	83333	38462
Mandibular bone	8000	0.31	7017.5	3053.4
Maxillary bone	2000	0.3	1666.7	769.23

3.Results and discussions

After the calculations were performed, the results were analyzed and the value tables were obtained for each considered calculation element.

A) Implants with large turns inserted at the mandibular level

The equivalent pressure varied between a minimum of 9.8508e-9MPa and a maximum of 27.741MPa, with an average of 2.5309MPa (Figure 2a).

The equivalent elastic relative deformation ranged from 1.5423e-003 mm/mm to 2.0501e-012 mm/mm, with an average of 1.1757e-004 mm/mm (Figure 2b).

The total deformation ranged from 0, a value recorded at the level of the palatal arch and in the interincisive area, up to a maximum of 5.9288e-003mm recorded in region 43, with an average of 2.2436e-003mm (Figure 2c).

Normal pressure ranged from -21.694MPa to 9.4MPa, with an average of -0.29378MPa (Figure 2d).

The shear stress on the XY axis ranged from -10.063MPa to 11.074MPa. The average value of the shear stress was 2.6217e-002MPa (Figure 2e).

On the YZ axis, the shear stress varied between -9.6772MPa and 8.7187MPa with an average of -1.2227e-002MPa (Figure 2f). On the XZ axis, the shear stress was between the limits -10.063MPa and 11.074MPa with an average of 2.6217e-002MPa (Figure 2g).

The deformation in the OX direction varied between -3.3131e-003mm and 1.2151e-003mm, with the average of -1.555e-004mm (Figure 2h). On the OY direction it ranged from -1.62e-003mm to 1.2504e-003mm, with an average of 3.2406e-004mm (Figure 2i). On the OZ direction it was between -5.7362e-003mm and 4.5881e-004mm, and the average was -1.9461e-003mm (Figure 2j).

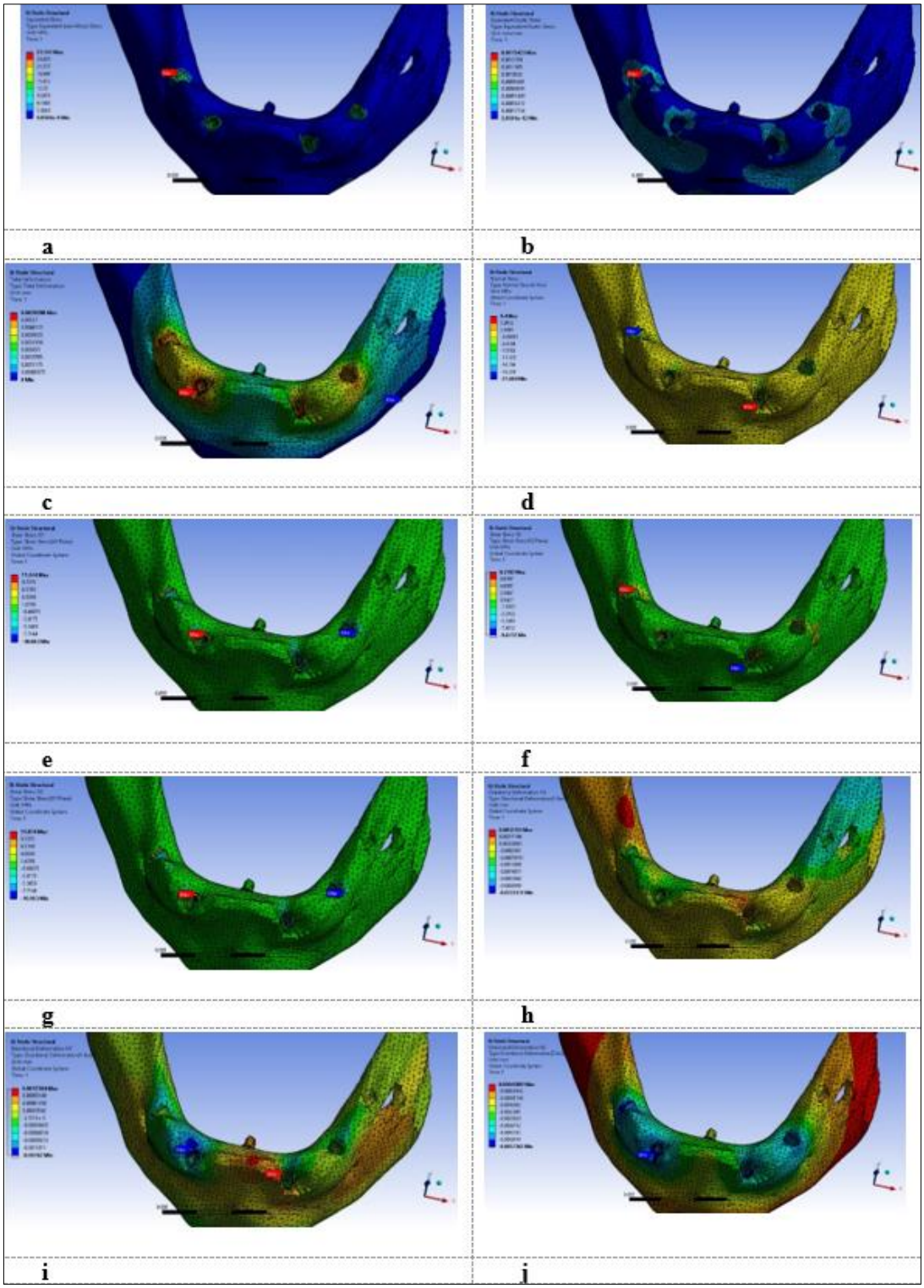

Figure 2, Simulations on the implants with large turns inserted at the mandibular level: a) Equivalent pressure; b) Equivalent elastic relative deformation; c) Total deformation; d) Normal pressure; e) Shear stress on the XY axis; f)- Shear stress on the YZ axis; g) Shear stress on the XZ axis; h) Deformation on the OX direction; i) Deformation on the OY direction; j) Deformation on the OZ direction

B) Implants with small turns inserted at the mandibular level

The equivalent pressure varied between a minimum of 8.4749e-008MPa and a maximum of 44.207MPa, with an average of 8.1404MPa (Figure 3a).

The equivalent elastic relative deformation ranged from 1.2144e-011 mm/mm to 1.3047e-003 mm/mm, with an average of 1.3043e-004 mm/mm (Figure 3b).

The total deformation ranged from 0mm, a value that was recorded at the mandibular basilar, up to a maximum of 8.9066e-003mm that was recorded at the neck-implant region, with an average of 3.5525e-003mm (Figure 3c).

Normal pressure varied between -17.621MPa and 12.342MPa, with an average of -0.30859MPa (Figure 3d).

The shear stress on the XY axis ranged from -10.108MPa to 10.709MPa. The average value of the shear stress was 7.3699e-002MPa (Figure 3e). On the YZ axis, the shear stress varied between -13.958MPa and 13.205MPa, with an average value of 0.33477MPa (figure 3f). On the XZ axis, the shear stress was between the limits -14.595MPa and 12.244MPa, the average being 0.39396MPa (Figure 3g).

The deformation on the OX direction varied between -3.5816e-003mm and 2.9764e-003mm, with an average of 2.7145e-004mm (Figure 3h). On the OY direction, the deformation varied between -5.1212e-003mm and 7.8937e-004mm, the average being -1.1834e-003mm (Figure 3i). On the OZ direction, the deformation was between -7.7482e-003 mm and 2.6033e-003 mm, and the average was -2.9909e-003mm (Figure 3j).

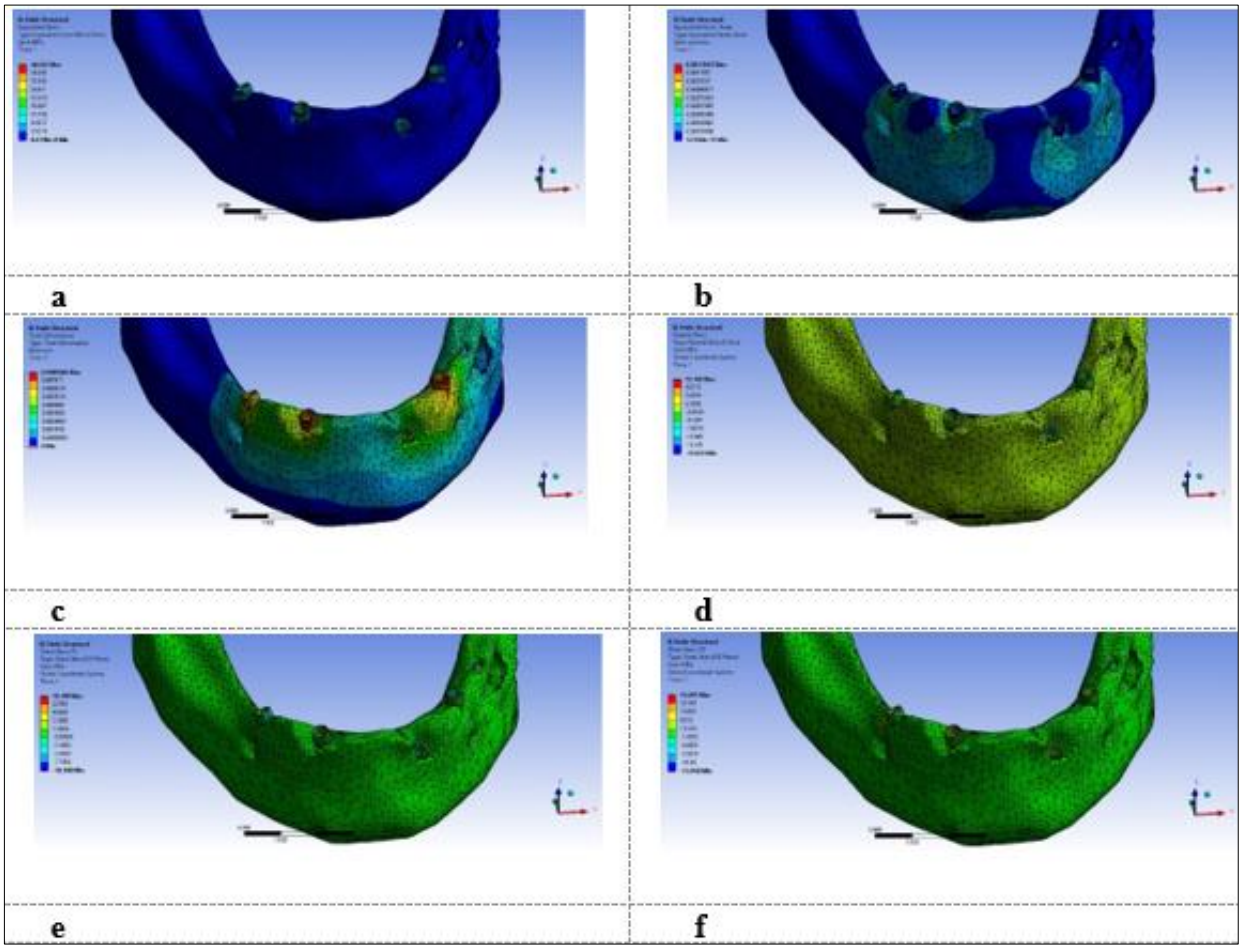

Figure 3. Simulations on the implants with small turns inserted at the mandibular level: a) Equivalent pressure; b) Equivalent elastic relative deformation; c) Total deformation; d) Normal pressure; e) Shear stress on the XY axis; f)- Shear stress on the YZ axis

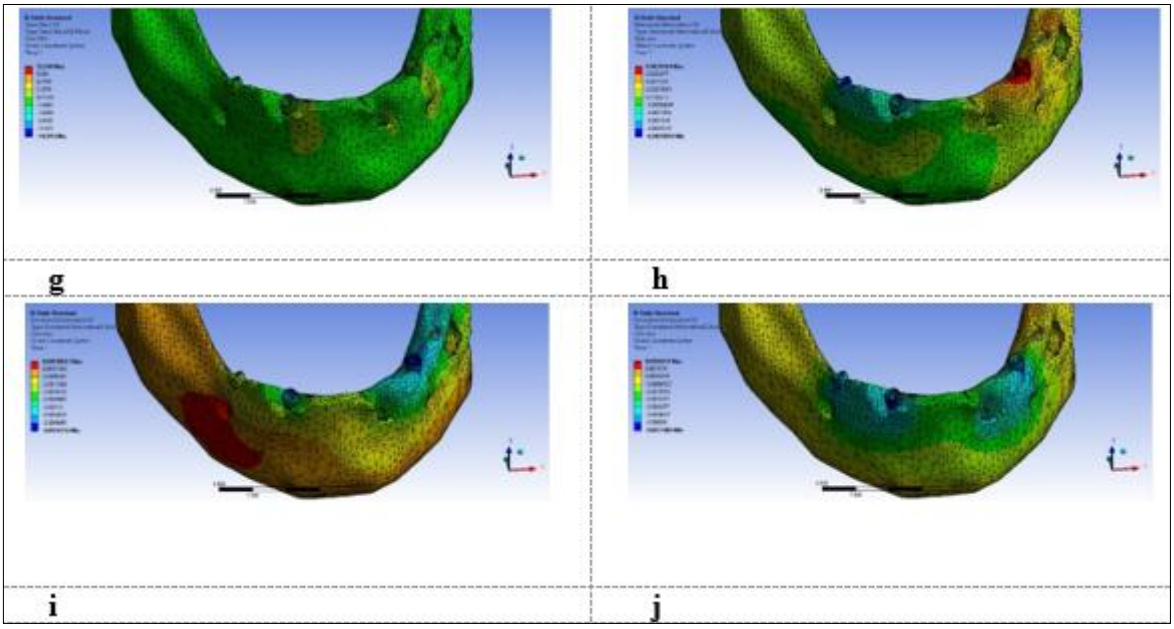

Figure 3. Simulations on the implants with small turns inserted at the mandibular level: g) Shear stress on the XZ axis; h) Deformation on the OX direction; i) Deformation on the OY direction; j) Deformation on the OZ direction

C) Implants with large turns inserted at the maxillary level

The equivalent pressure (von-Mises) varied between a minimum of 0 MPa and a maximum of 164.63MPa, with an average of 6.1385MPa (Figure 4a). The minimum pressure was recorded in quadrant 1, and the maximum pressure in quadrant 2.

The equivalent elastic relative deformation ranged from 0 mm/mm to 2.3021e-002 mm/mm, with an average of 8.4697e-004 mm/mm (Figure 4b).

The total deformation ranged from 0, a value that was recorded at the alveolar ridge, up to a maximum of 7.9164e-002mm that was recorded at the tuberosity region, with an average of 1.7599e-002mm (Figure 4c).

Normal pressure varied between -79.126MPa and 94.987MPa, with an average of -0.24352MPa (Figure 4d).

The shear stress on the XY axis ranged from -45.285MPa to 29.741MPa. The average value of the shear stress was -5.2877e-002MPa (Figure 4e). The shear stress on the YZ axis varied between a minimum of -35.4MPa and a maximum of 49.214MPa, with an average of -0.43694MPa (Figure 4f). The shear stress on the XZ axis had a minimum of -54.284MPa and a maximum of 35.008MPa, with an average of -5.3712e-002MPa (Figure 4g).

Deformation on the OX axis was between -4.9018e-002mm and 2.5572e-002mm, with an average of -2.8357e-003mm (Figure 4h). Deformation on the OY axis started from a minimum of -4.935e-002mm and reached a maximum of 1.0814e-002mm, with an average value of -6.612e-003mm (Figure 4i). The deformation on the OZ axis was between -8.236e-003mm and 6.2531e-002mm, with an average of 1.2931e-002mm (Figure 4j).

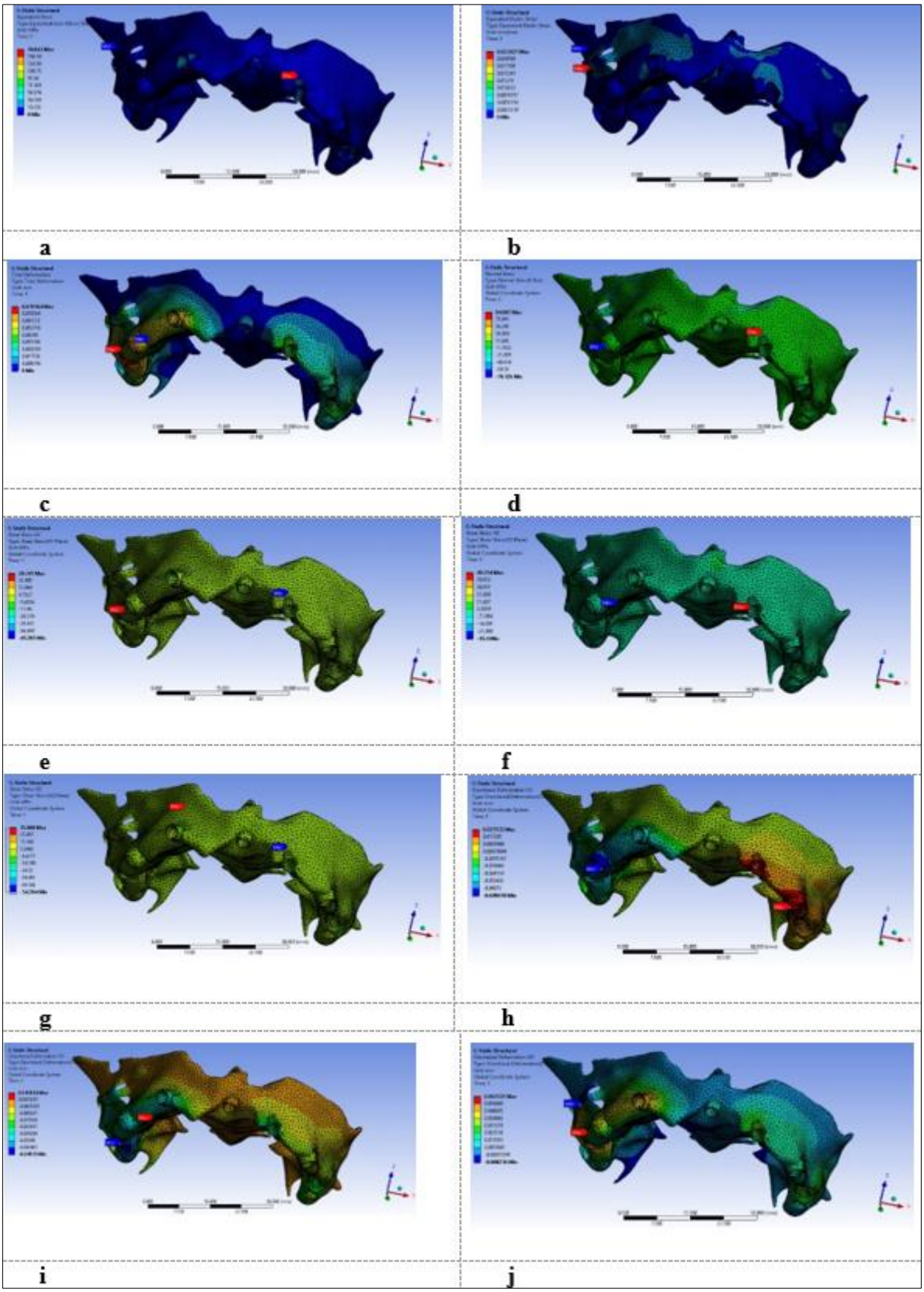

Figure 4. Simulations on the implants with large turns inserted at the maxillary level: a) Equivalent pressure; b) Equivalent elastic relative deformation; c) Total deformation; d) Normal pressure; e) Shear stress on the XY axis; f)- Shear stress on the YZ axis; g) Shear stress on the XZ axis; h) Deformation on the OX direction; i) Deformation on the OY direction; j) Deformation on the OZ direction

D) Implants with small turns inserted at the maxillary level

The equivalent pressure varied between a minimum of 1.6955e-008MPa and a maximum of 152.72MPa, with an average of 6.582MPa (Figure 5a). Both minimum and maximum pressures, were recorded on the left side of the maxillary bone.

The equivalent elastic relative deformation ranged from 1.2817e-011 mm/mm to 6.6081e-002 mm/mm, with an average of 8.9815e-004 mm/mm (Figure 5b).

The total deformation ranged from 0, a value that was recorded at the palatal arch level and into the interincisive area, up to a maximum of 7.7897e-002 MPa recorded in region 17, with an average of 1.8153e-002 MPa (Figure 5c).

Normal pressure varied between -102.23MPa and 31.778MPa, with an average of -0.1761MPa (Figure 5d).

The shear stress on the XY axis varied between -29.485MPa and 37.224MPa (Figure 5e). The average value of shear stress was -8.6255e-003MPa. On the YZ axis, the shear stress varied between -68.034MPa and 38.272MPa (Figure 5f). On the XZ axis, the shear stress was between the limits -35.287 MPa and 43.761 MPa (Figure 5g).

The deformation on the OX direction varied between -4.8745e-002mm and 2.575e-002mm (Figure 5h). On the OY direction it varied between -5.1879e-002 mm and 1.2377e-00 mm (Figure 5i). On the OZ direction it was between -1.5383e-002 mm and 5.9813e-002 mm (Figure 5j).

Studies have shown that, during the first year after implant insertion, an approximately 1 mm vertical bone loss will occur, followed frequently by an additional bone loss of 0.1mm on each subsequent year. [23, 24]

This marginal bone loss can be mainly caused by microbial accumulation around the implant and periimplantar tissues, or by inadequate mechanical stimuli [25].

Attempts have focused on increasing the diameter and / or length of the implants or modifying their design, in order to increase the contact area between the bone and the implant and to reduce stress into the periimplantar bone [26].

Some researchers [27] consider that the diameter of the implant is the most important factor that dictates the reduction of stresses and deformations in the periimplantar bone, while others [28] consider that the length of the implant has a greater impact on the distribution of stress in the periimplantar bone. On the other hand, it has been shown that neither the diameter of the implant, nor its length are as important as the surgical insertion technique, adequate primary stability and pre- and postoperative oral hygiene. [29]

Larger implants, in both diameter and length, has been shown to improve the distribution patterns of stresses and deformations; however, in many clinical situations, the alveolar bone does not have sufficient thickness or height to insert such implants. [26]

Finite element analysis (FEA) allows researchers to appreciate the pattern of stress and strain distribution in the periimplantar bone. [30]

Several clinical studies have shown that, on a long term, the success of small diameter implants is less frequent than standard diameter implants [31, 32]. A recent prospective study evaluated small diameter implants, that were monitored for 5 years, clinically and radiologically, and explained that the use of two 3mm narrowing implants, is useful for stable marginal bone [33].

Other studies [34, 35] have shown that insertion of larger diameter implants is favorable for the long-term maintenance of the bone-implant interface in optimal conditions.

At equal demands on each implant, there are differences between the distribution of stresses and deformities into the maxillar and mandible, both because of the different characteristics of the two bones, mentioned in other studies [36], due to the fact that only 4 implants were possible on the mandible , while on the maxillar were possible 7 implants. Obviously, the positioning was imposed by the use of a real case with total edentation and different bone loss along the two arches. The 2 pterygoid implants, by the nature of their strongly inclined position, will determine demands on all 3 directions of the coordinate axes.

Principled, the appearance of some request that change its sign - there are also areas with zero demand – it has the effect of producing a twisting of the element in which this pressure sign change appears, element named bone, which also has the weakest behavior from the mechanical point of view.

4.Conclusions

1) Regardless of the type of implant and regardless of the maxillary or mandibular area where the implants were virtually inserted, the critical areas in which extreme values are developed, are located into the bone at the neck-implant level and its apex level.

2) The tensions and deformations developed in our study does not present values that theoretically could endanger the osseointegration of the implants, but if they occur for long periods of time, they can induce fatigue of the bone substrate in the critical areas.

3) Implants with small turns induce lower stresses and deformations, compared to implants with large turns, regardless of the arch in which they were inserted on.

References

1CICCIU, M., et al, Materials, **11**, 2018, p. 1512; doi:10.3390/ma11091512.
2.CERVINO, G., et al. Open Dent. J., **12**, 2018, p. 219.
3.LAURITANO, F., et al, Minerva Stomatol., **65**, 216, p. 353.
4.CICCIÙ, M., et al, Minerva Stomatol., **58**, 2009, p. 9.
5.BRAMANTI, E., et al, Sci. World J., Volume 2017, Article ID 1029574, 7 pages, https://doi.org/10.1155/2017/1029574.
6.YASHWANT, A.V., et al. Journal of Clinical and Diagnostic Research **11.5**, 2017: ZC17-ZC20.
7.KÜÇÜKKURT, S., et al. Computer Methods in Biomechanics and Biomedical Engineering **20.3**, 2017, p. 284.
8.YAZICIOGLU, D., et al. Journal of Oral Implantology **42.1**, 2016, p. 26.
9.SOTTO-MAIOR, B.S., et al. Computer Methods in Biomechanics and Biomedical Engineering **19.7**, 2016, p. 699.
10.MARKOSE, J., et al. Journal of Contemporary Dental Practice **18.6**, 2017, p. 510.
11.ARADYA, A., et al. Indian Journal of Dental Research **27.1**, 2016, p. 78.
12.SESHA REDDY, M., et al. EC Dental Science **17.11**, 2018, p. 1950.
13.OMORI, M., et al. International Journal of Implant Dentistry **1.1**, 2015, p. 10.
14.DETOLLA, D.H., et al. Journal of Oral Implantology **26.2**, 2016, p. 77.
15.COMANEANU, R.M., BARBU, H.M., VLASCEANU, D., TARCOLEA M., Key Engineering Materials, vol **583,** 2014, p. 169.
16.ORMENISAN, A., TARCOLEA, M., SUCIU, M., GRIGORAS, R.I., BERESESCU, F.G., VLASCEANU, G., HANCU, V., COMANEANU, R.M., *Mater. Plast.*, **52**(3), 2015, 373.
17.COMAN, C., GHERGIC, D.L., PATROI, D.N., TARCOLEA, M., COMANEANU, R.M., BARBU, H.M., *Mater. Plast.*, **53**(1), 2016, 91.
18.COSARCA, A.S., GRIGORAS, R., HANCU, V., COMAN, C., COMANEANU, R.M., et al, *Mater. Plast.*, **53**(1), 2016, p. 135.
19.BERESESCU, G., ORMENISAN, A., COMANEANU, R.M., et al, *Mater. Plast.*, **55**(1), 2018, p. 42.
20.DRAGUS, L., TINU, A.S., COMAN, C., COMANEANU, R.M., GHERGIC, D.L., *Rev. Chim.* **69**(9), 2018, 2594.
21.COMANEANU, R.M., BORDEA, L.E., PARASCHIV, V., BOTOACA, O., BECHIR, F., TARCOLEA, M., COMAN, C., TANASE, M., *Rev. Chim.*, **70**(1)1, 2019, 74.
22.ESPOSITO, M., HIRSCH, J.M., et al, Eur. J. Oral Sci. **106**, 1998, p. 721.
23.COCS, J.F., ZARB, G.A., Int J Oral Maxillofac Implants., **2**, no. 2, 1987, p. 91.
24.KIM, Y.T., LIM, G.H., et al, J Periodontal Implant Sci., **47**, no. 4, 2017, p. 231.
25.PEIXOTO, C.D., ALMAS, K. et al, Odontostomatol Trop., **39**, no. 153, 2016, p. 23.
26.UEDA, N., et al, J Prosthodont Res., **61**, no. 3, 2017, p. 324.

27.VAIRO, G., SANNINO, G., Comput Math Methods Med. Volume 2013, Article ID 250929, 15 pages, http://dx.doi.org/10.1155/2013/250929.
28.GUAN, H., et al, Int J Oral Maxillofac Implants., **24**, no. 5, 2009, p. 866.
29.JAVED, F., ROMANOS, G.E., Clin Oral Investig., **19**, no. 1, 2015, p.1–10.
30.SUGIURA, T., et al, Med Oral Patol Oral Cir Bucal., **20**, no. 1, 2015, e66.
31.LEE, C.T., et al, Clin Oral Implants Res., **27**, no. 10, 2016, p. 1251.
32.ZWEERS, J., et al, Clin Oral Implants Res., **26**, no. 2, 2015, p. 149.
33.GALINDO-MORENO, P., et al. Clin Oral Implants Res., **28**, no. 12, 2017, p. 1584.
34.OHYAMA, T., YASUDA, H., SHIBUYA, N., et al. J Oral Sci., **59**, no. 2, 2017, p. 273.
35.JAFARIAN, M., et al, Dent Med Probl., **56**, no. 1, 2019, p. 27.
36.CERVINO, G., et al. Open Dent J. **12**, 2018, p. 219

Manuscript received: 16.12.2019